

## Effect of membrane tension on transbilayer movement of lipids

メタデータ	言語: eng 出版者: 公開日: 2019-06-26 キーワード (Ja): キーワード (En): 作成者: Hasan, Moynul, Saha, Samiron Kumar, Yamazaki, Masahito メールアドレス: 所属:
URL	<a href="http://hdl.handle.net/10297/00025405">http://hdl.handle.net/10297/00025405</a>

# Effect of membrane tension on transbilayer movement of lipids

Moynul Hasan,<sup>1</sup> Samiron Kumar Saha,<sup>1</sup> and Masahito Yamazaki<sup>1,2,3,a)</sup>

<sup>1</sup>*Integrated Bioscience Section, Graduate School of Science and Technology, Shizuoka University, Shizuoka 422-8529, Japan*

<sup>2</sup>*Nanomaterials Research Division, Research Institute of Electronics, Shizuoka University, 836 Oya, Suruga-ku, Shizuoka 422-8529, Japan*

<sup>3</sup>*Department of Physics, Faculty of Science, Shizuoka University, Shizuoka 422-8529, Japan*

(Received 13 April 2018; accepted 8 June 2018; published online 26 June 2018)

The stretching of plasma membranes of cells and lipid bilayers of vesicles affects the physical properties of the membrane as well as the functions of proteins/peptides in the membranes. Here, we examined the effect of membrane tension on the rate constant of the transbilayer movement ( $k_{FF}$ ) of fluorescent probe-labeled lipids using a new method. Specifically, we recently reported [Hasan *et al.*, *Langmuir* **34**, 3349 (2018)] the development of a technique that employs giant unilamellar vesicles (GUVs) with asymmetric lipid compositions in two monolayers. In the present work, we found that the  $k_{FF}$  greatly increased with tension without leakage of water-soluble fluorescent probes from the GUV lumen (i.e., without the formation of pores in the GUV membrane). We discussed the plausible mechanisms for the effect of tension on the transbilayer movement of lipids. As one of the mechanisms, we hypothesized that the transbilayer movement of lipids occurs through the lateral diffusion of lipids in the walls of hydrophilic pre-pores. *Published by AIP Publishing.* <https://doi.org/10.1063/1.5035148>

## I. INTRODUCTION

Several external factors such as forces,<sup>1,2</sup> electric fields,<sup>3</sup> and osmotic pressure<sup>4</sup> produce lateral membrane tension in the plasma membranes of cells and the lipid bilayers of vesicles, inducing stretching and compression of these membranes. It is well known that this stretching affects the physical properties of the membranes as well as the functions of membrane proteins.<sup>5</sup> For example, if this stretching reaches a large enough value, pore formation occurs in the membranes, resulting in rupturing of the vesicles and cells. The tension-induced pore formation and rupture of vesicles have been investigated using giant unilamellar vesicles (GUVs).<sup>1-4,6-9</sup>

Theorizing about tension-induced pore formation has led to the development of the following well-recognized model.<sup>10-12</sup> Thermal fluctuations of lipid bilayers are believed to induce various transient rarefactions (i.e., areas of the lower lipid density). As one of these rarefactions, a hydrophilic pre-pore with the toroidal structure has been proposed,<sup>7-12</sup> wherein the outer and inner monolayers bend and merge with each other in a toroidal fashion to form a pore in which the inner wall is composed primarily of the hydrophilic segments of lipid molecules. This pre-pore is unstable because the edge of the pre-pore has a high free energy and thus rapidly closes. In this way, thermal energy induces a fluctuation of the radius of the pre-pore; if a pre-pore overcomes the activation energy (or the energy barrier) of pore formation, the pre-pore transforms into a pore. If the tension increases, the activation energy decreases and thus the rate constant of the tension-induced rupture of a vesicle increases. Although

this theory can reasonably explain the experimental results of the tension-induced rupture of vesicles,<sup>2,7-9</sup> experimental evidence for the existence of the pre-pores is limited. One indication for the existence of pre-pores is the fluctuation of conductance in a planar lipid bilayer containing decane and octane.<sup>13</sup> However, the use of GUVs to obtain experimental evidence for pre-pores has not yet (to our knowledge) been reported.

In this report, we employed another method to investigate the existence of pre-pores. It is known that the rate of transbilayer movement (i.e., flip-flop) of lipid molecules with large charged hydrophilic segments (i.e., polar head groups) is usually very small ( $\sim 10^{-5} \text{ s}^{-1}$  depending on the kinds of lipids and temperature) because the translocation of the charged segments across the hydrocarbon core of the lipid membrane is energetically unfavorable.<sup>14-18</sup> However, if hydrophilic pre-pores exist in the lipid bilayers, these lipid molecules are expected to diffuse laterally through the wall of the pre-pore, thereby increasing the rate of transbilayer movement of these lipids. Recently, we reported the development of a new method to estimate the rate constant of the transbilayer movement of lipids in single GUVs, specifically by using GUVs with asymmetric lipid compositions in two monolayers.<sup>19</sup> This method enables observation of the elementary processes of transbilayer movement and also facilitates measurement of the effect of tension on transbilayer movement. Therefore, in the present report, we used this new method to examine the effect of tension on the rate constant of the transbilayer movement of several fluorescent probe-labeled lipids, including 1-oleoyl-2-{6-[(7-nitro-2-1,3-benzoxadiazole-4-yl) amino] hexanoyl}-*sn*-glycero-3-phospho-*rac*-(1-glycerol) (18:1-06:0 NBD-PG; hereafter NBD-PG). The movement of these lipids was evaluated

<sup>a)</sup>Author to whom correspondence should be addressed: yamazaki.masahito@shizuoka.ac.jp. Tel./FAX: 81-54-238-4741.

in GUVs composed of dioleoylphosphatidylcholine (DOPC) and dioleoylphosphatidylglycerol (DOPG).

## II. MATERIALS AND METHODS

DOPG, DOPC, NBD-PG, 1-oleoyl-2-hydroxy-*sn*-glycero-3-phosphoethanolamine-N-(7-nitro-2-1,3-benzoxadiazole-4-yl) (18:1-NBD-lyso-PE; hereafter NBD-LPE), and 1,2-dioleoyl-*sn*-glycero-3-phosphoethanolamine-N-(7-nitro-2-1,3-benzoxadiazole-4-yl) (18:1 NBD-PE; hereafter NBD-PE) were purchased from Avanti Polar Lipids, Inc. (Alabaster, AL). Alexa Fluor 647 (AF647) hydrazide was purchased from Invitrogen, Inc. (Carlsbad, CA). Bovine serum albumin (BSA) was purchased from Wako Pure Chemical Industry, Ltd. (Osaka, Japan).

GUVs of DOPG/DOPC/NBD-PG (40/(60- $x$ )/ $x$ ; molar ratio) (hereafter, PG/PC/NBD-PG), DOPG/DOPC/NBD-LPE (40/(60- $x$ )/ $x$ ; molar ratio) (hereafter, PG/PC/NBD-LPE), and DOPG/DOPC/NBD-PE (40/(60- $x$ )/ $x$ ; molar ratio) (hereafter, PG/PC/NBD-PE) were prepared in buffer A [10 mM PIPES, pH 7.0, 150 mM NaCl, and 1 mM egtazic acid (EGTA)] containing 0.10 M sucrose by the natural swelling method.<sup>19</sup> To prepare GUVs containing AF647 in their lumens, we used buffer A containing 6  $\mu$ M AF647 and 0.10 M sucrose in the above procedure. To obtain a purified GUV suspension in buffer A containing 0.10 M glucose, smaller vesicles and the untrapped fluorescent probe were removed using the membrane-filtering method.<sup>20</sup> The methods for the observation of GUVs at  $25 \pm 1$  °C using confocal laser scanning microscopy (CLSM) and for the analysis of the fluorescence intensity (FI) of the GUV membranes were described previously.<sup>19</sup>

To apply tension,  $\sigma$ , to the lipid membrane of single GUVs, we used the standard micropipette aspiration method.<sup>8,9,21</sup>  $\sigma$  is controlled as a function of the aspiration pressure  $\Delta P$ , i.e., the pressure difference between the outside and the inside of the micropipette is as follows:<sup>21</sup>

$$\sigma = \frac{\Delta P d_p}{4(1 - d_p/D_V)}, \quad (1)$$

where  $d_p$  is the internal diameter of the micropipette and  $D_V$  is the diameter of the spherical cap segment (on the outside of the micropipette) of the aspirated GUV. The method of the application of tension to individual GUV was described previously.<sup>8,9</sup> During the application of the constant tension, we measured the FI of the individual GUV lumen and rim.

## III. RESULTS

First, we prepared GUVs with the asymmetric distribution of NBD-PG (whose NBD group is attached with its hydrocarbon chain), i.e., PG/PC/NBD-PG (inner monolayer) and PG/PC (outer monolayer), using our previously reported method.<sup>19</sup> In this method, we prepared GUVs with symmetric lipid compositions of PG/PC/NBD-PG (40/59/1) in buffer A and then removed NBD-PG from the outer monolayers of these GUVs by continuously replacing the buffer surrounding the GUVs with a new buffer using the membrane-filtering

method.<sup>20</sup> The critical micelle concentration (CMC) of NBD-PG is 0.3  $\mu$ M (obtained using the method described in our paper),<sup>19</sup> which is similar to the value for 16:0-06:0 NBD-PC (0.2  $\mu$ M).<sup>22</sup> Hence, we reasonably expected that the NBD-PG in the outer monolayer was rapidly transferred into the aqueous solution. Figures 1(a) and 1(b) show the representative CLSM images of one of the PG/PC/NBD-PG (40/59/1)-GUVs before and after (respectively) 1 h of purification. These images indicated that the FI of the GUV membrane (i.e., the rim intensity) due to NBD-PG after purification was smaller than that before purification. We measured the rim intensity of multiple GUVs and obtained rim intensities (mean  $\pm$  SD) before and after purification of  $2890 \pm 140$  ( $n = 14$  examined GUVs) and  $1530 \pm 110$  ( $n = 12$ ), respectively. The ratio of the FI after purification to that before purification was 0.52. This result indicated that the concentration of NBD-PG in the GUV membrane was approximately halved by purification.

To confirm whether the unbinding of NBD-PG from the outer leaflet to aqueous solution is rapid, we investigated the interaction of the buffer with a single PG/PC/NBD-PG (40/59/1)-GUV before purification. First, we selected a PG/PC/NBD-PG (40/59/1)-GUV under the CLSM, and then the buffer in the neighborhood of this GUV was continuously replaced by the flow of a new buffer through the micropipette. The rim intensity gradually decreased with time, achieving a plateau of approximately half the original intensity after  $\sim 1500$  s [Fig. 1(c)]. The decrease in the rim intensity after 300 s was fit to an exponential decay function, yielding a rate constant of unbinding (i.e., transfer) of NBD-PG from the monolayer to aqueous solution ( $k_{\text{unbind}}$ ) of  $2.5 \times 10^{-3} \text{ s}^{-1}$ .

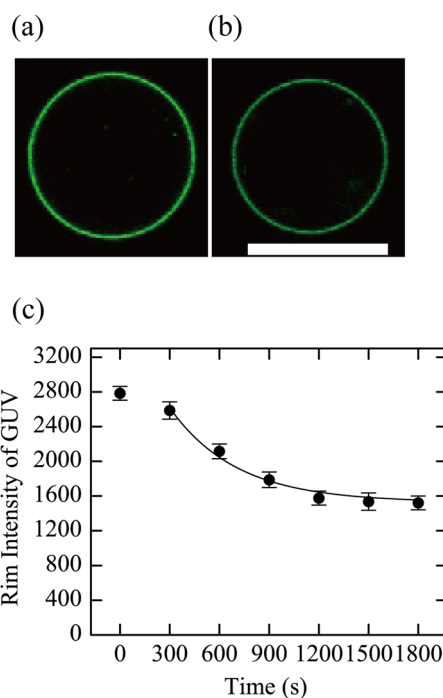


FIG. 1. CLSM images of PG/PC/NBD-PG (40/59/1)-GUVs. (a) One of the GUVs before purification and (b) one of the GUVs after purification. The bar represents 20  $\mu$ m. (c) The effect of interaction of a GUV with a new buffer provided through a micropipette on its rim intensity.

The mean value and SD of  $k_{\text{unbind}}$  were  $(2.5 \pm 0.2) \times 10^{-3} \text{ s}^{-1}$  ( $n = 6$ ). This result implied that the unbinding of NBD-PG from the outer leaflet to aqueous solution occurred during the purification and further indicated that the NBD-PG concentration in the outer leaflet was almost zero after 1 h of purification. Moreover, NBD-PG has a large binding constant to the membrane due to the presence of long hydrocarbon chains. As discussed in our previous paper,<sup>19</sup> in this case, the amount of unbinding of NBD-PG from the inner leaflet to the aqueous solution of the GUV lumen was negligible; hence, the NBD-PG concentration in the inner leaflet did not change during the purification (i.e., 1 mol. %). Based on these results, we concluded that we succeeded in preparing GUVs with asymmetric distribution of NBD-PG, i.e., PG/PC/NBD-PG (40/59/1; inner monolayer)-PG/PC (40/59; outer monolayer)-GUVs.

Using these asymmetric GUVs, we estimated the rate constant of transbilayer movement of NBD-PG from the inner monolayer to the outer one in the GUVs under various membrane tensions at 25 °C. Figure 2(a) shows the

time course of the rim intensity of PG/PC/NBD-PG (40/59/1; inner monolayer)-PG/PC (40/59; outer monolayer)-GUVs after purification (in the absence of tension). The rim intensity decreased by 3% after 2 h of observation using CLSM. Next we applied a membrane tension of 6.0 mN/m to a PG/PC/NBD-PG (40/59/1; inner)-PG/PC (40/59; outer)-GUV containing the water-soluble fluorescent probe AF647 inside the GUV lumen [Fig. 2(b)] and observed the time courses of the FI of the GUV lumen and the rim intensity. Figure 2(c) shows that the FI of the GUV lumen due to AF647 was constant up to 184 s, indicating no pore formation in the GUV membrane through which AF647 leaked and then rapidly decreased to zero. As shown in our previous paper,<sup>23</sup> this sudden change reflects the aspiration of the GUV into the micropipette after the tension-induced rupture of the GUV owing to pore formation in the GUV membrane. The rim intensity due to NBD-PG decreased linearly with time until the rupture of the GUV. In some cases, the rupture of the GUV did not occur for 6 min, whereas the rim intensity due to NBD-PG decreased with time until 6 min without leakage of AF647 [Fig. 2(d)].

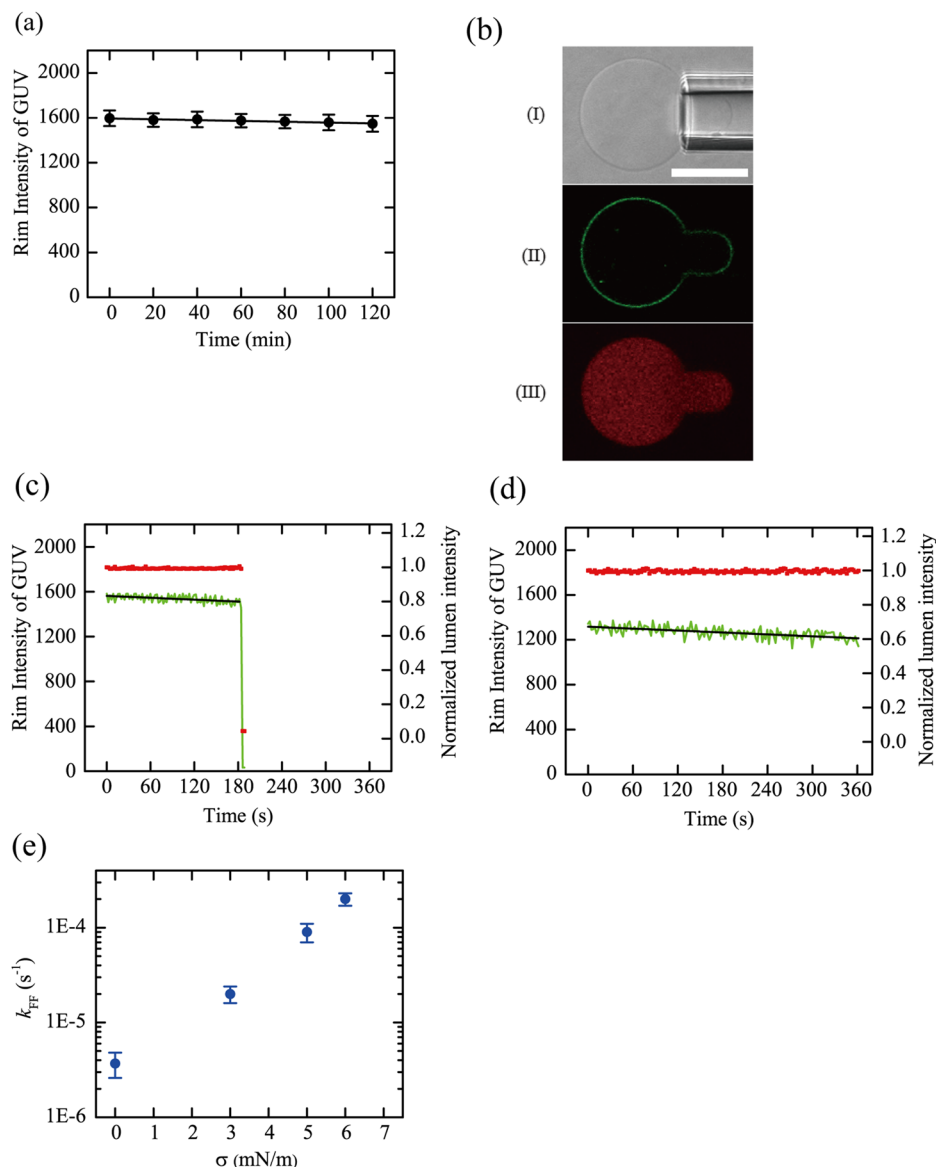


FIG. 2. Effect of tension on the time course of the rim intensity of PG/PC/NBD-PG (40/59/1; inner)-PG/PC (40/59; outer)-GUVs at 25 °C. (a)  $\sigma = 0 \text{ mN/m}$ . (b) Microscopic images of the GUV aspirated by a micropipette. CLSM images of (I) DIC, (II) NBD-PG, and (III) AF647. The bar represents  $20 \mu\text{m}$ . (c) and (d)  $\sigma = 6 \text{ mN/m}$ . The GUVs contained AF647 inside their lumen. The red squares indicate the FI of the GUV lumen due to AF647, and the green line indicates the rim intensity due to NBD-PG. The black solid lines show the best-fit curve using Eq. (2). (e) Dependence of  $k_{\text{FF}}$  on tension. Mean values and SDs of  $k_{\text{FF}}$  for each tension are shown.

It is generally recognized that the transbilayer movement of lipids follows first-order reaction kinetics,<sup>14–18</sup> and thus, the concentration of NBD-PG in the inner monolayer,  $C(t)$ , decreases exponentially. If we denote the rate constant of the transbilayer movement of lipids (here, NBD-PG) as  $k_{FF}$ , then  $C(t) = C(0) \exp(-k_{FF}t)$ , where the  $C(0)$  is  $C(t)$  at  $t = 0$ . Generally, the rim intensity of the GUV membrane,  $I(t)$ , is proportional to the NBD-PG concentration in the membrane. In the present experiment,  $I(t)$  is determined by two elementary processes: the transbilayer movement of NBD-PG from the inner leaflet to the outer leaflet and the unbinding of NBD-PG from the outer leaflet to aqueous solution outside the GUV. If the rate of the former process is much smaller than that of the latter one, i.e., the transbilayer movement is the rate-limiting step,  $I(t)$  is determined primarily by the transbilayer movement of NBD-PG and therefore is described by the following equation:

$$I(t) \approx I(0) \exp(-k_{FF}t) \approx I(0)(1 - k_{FF}t), \quad (2)$$

where the final equation is the approximate one for  $k_{FF} \ll 1$ . The time courses of the rim intensities could be fit well to Eq. (2), yielding  $k_{FF}$  values of  $1.8 \times 10^{-4} \text{ s}^{-1}$  and  $2.2 \times 10^{-4} \text{ s}^{-1}$  for Figs. 2(c) and 2(d), respectively. We performed the same experiments with multiple GUVs and obtained  $k_{FF} = (2.0 \pm 0.3) \times 10^{-4} \text{ s}^{-1}$  ( $n = 15$ ). Using the same method, we obtained the values of  $k_{FF}$  of NBD-PG under various tensions. Figure 2(e) shows that  $k_{FF}$  increased with tension.

Next, we investigated the  $k_{FF}$  of different kinds of lipids. First, we attempted the preparation of GUVs with the asymmetric distribution of NBD-PE (whose NBD group is attached with its headgroup). The rim intensity values of multiple PG/PC/NBD-PE (40/59/1)-GUVs before and after purification were  $3570 \pm 170$  ( $n = 11$ ) and  $3520 \pm 130$  ( $n = 15$ ), respectively. These values did not differ significantly, indicating that the NBD-PE in the outer monolayer did not transfer into the aqueous solution after 1 h, probably due to its lower CMC value.<sup>24</sup> Instead, we used NBD-LPE (whose NBD group is attached with its headgroup) with a hydrocarbon chain. We prepared PG/PC/NBD-LPE (40/59/1; inner monolayer)-PG/PC (40/59; outer monolayer)-GUVs using the method described previously.<sup>19</sup> We measured the rim intensity of a single PG/PC/NBD-LPE (40/59/1; inner)-PG/PC (40/59; outer)-GUV in the absence of tension for 15 min, and this time course was fit to Eq. (2). The  $k_{FF}$  for  $\sigma = 0$  was  $(4.3 \pm 1.0) \times 10^{-6} \text{ s}^{-1}$  ( $n = 5$ ), which does not differ significantly from the value obtained by an intermittent measurement of the rim intensity for 2 h with brief exposure to light.<sup>19</sup> This result indicated that photobleaching of NBD-LPE was negligible under the condition of 15 min of light exposure. Next, we applied a tension of 5.0 mN/m to a GUV of the same lipid composition but containing AF647 and observed the time course of the rim intensity. Figure 3(a) indicates that the rim intensity due to NBD-LPE decreased with time for 15 min without leakage of AF647, a time course that could be fit well to Eq. (2). This analysis yielded a value for  $k_{FF}$  of  $(5.0 \pm 1.0) \times 10^{-5} \text{ s}^{-1}$  ( $n = 7$ ). Figure 3(b) shows that the  $k_{FF}$  of NBD-LPE increased with tension and that these  $k_{FF}$  values were a little smaller than those of NBD-PG.

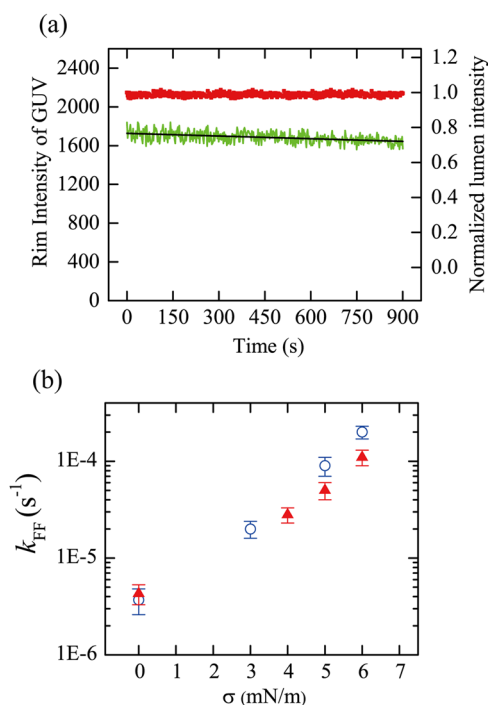


FIG. 3. Effect of tension on the time course of the rim intensity of PG/PC/NBD-LPE (40/59/1; inner)-PG/PC (40/59; outer)-GUVs at 25 °C. (a)  $\sigma = 5$  mN/m. The red squares indicate the FI of the GUV lumen due to AF647, and the green line indicates the rim intensity due to NBD-LPE. The black solid line shows the best-fit curve using Eq. (2). (b) Dependence of  $k_{FF}$  on tension ( $\blacktriangle$ ). For comparison, the dependence of  $k_{FF}$  of NBD-PG on tension [Fig. 2(e)] was also plotted ( $\circ$ ). Mean values and SDs of  $k_{FF}$  for each tension are shown.

#### IV. DISCUSSIONS

These results indicated that the  $k_{FF}$  of lipids increased with membrane tension without leakage of AF647 (i.e., no pore formation). The  $k_{FF}$  of NBD-PG at 6 mN/m was  $\sim 50$  times larger than that in the absence of tension. To the best of our knowledge, these results are the first experimental evidence of the effect of tension on the transbilayer movement of lipids in lipid bilayers.

Here we consider the plausible mechanisms for the increase in transbilayer movement of lipids in the bilayer induced by tension. Under normal conditions, the transbilayer movement of lipids in lipid bilayers is believed to occur via transbilayer diffusion.<sup>14–18</sup> In this case, the transition state of the transbilayer diffusion of lipids is the state where the headgroups of lipids are located in the center of the hydrophobic core of the bilayer, which has a low dielectric constant.<sup>18</sup> Since the headgroups have a few charges, the electrostatic free energy (i.e., the Born energy) of the lipids in the transition state is large, which increases the activation energy of the transbilayer diffusion. The nature of the structure of the hydrocarbon chain of a lipid also affects the rate constant of transbilayer diffusion of the lipid, but the effect of this structure is not as large ( $\sim 2$  fold).<sup>18</sup> It is difficult to conceive of how the tension or the accompanying stretching of the lipid bilayer would greatly change the dielectric constant of the central region of the bilayer. Recent molecular dynamics (MD) simulations indicate that positively charged arginine translocates through

the hydrophobic core of the lipid bilayer by forming a water-filled defect that keeps the arginine molecule hydrated in the membrane.<sup>25</sup> In the case of the transbilayer diffusion of lipids, there may be a similar mechanism for the translocation of the charged headgroup across the hydrophobic core to prevent an increase in free energy due to the Born energy. Hence, the transbilayer movement of lipids in the bilayer may occur with  $k_{FF}$  of  $\sim 10^{-5} \text{ s}^{-1}$ . It is recently reported that the membrane stretching due to lateral tension increases the fluidity of lipid bilayers<sup>26,27</sup> and diffusion coefficient of lipid molecules,<sup>26–28</sup> which might facilitate the formation of a water-filled defect, resulting in an increase in  $k_{FF}$  of lipids.

Alternatively, we can consider this new phenomenon from a different point of view that the transbilayer movement of lipids may occur through pores and pre-pores. Here, we define a pore as a water channel in a lipid bilayer that is always open and whose diameter is sufficiently large so that fluorescent probes can pass through the pore and define a pre-pore as a transient small-sized pore through which the fluorescent probes cannot permeate. We explain the pre-pore in more detail as follows. In the liquid-crystalline ( $L_\alpha$ ) phase, the thermal fluctuation of the structure of the lipid bilayers is large, resulting in a transient decrease in the lateral density of lipid bilayers (i.e., rarefaction) at some local areas. Hence we can expect that various structures of rarefactions appear transiently in the membranes. When the size of a rarefaction reaches a critical value, it becomes a hydrophilic pre-pore [Fig. 4(aI) or 4(bI)].<sup>7–12,29–31</sup> As the radius of the pre-pore increases, the radius of the water channel at the center of the pre-pore increases [Fig. 4(aII) or 4(bII)]. Hence, water molecules can permeate through a pre-pore, but its rate may be slow due to the small lifetime of the pre-pore (see the details later). It is believed that the hydrophilic pre-pore has the toroidal structure whose wall contacting water is mainly composed of the hydrophilic segments of lipid molecules (Fig. 4).<sup>30,31</sup> However, it is difficult to determine experimentally the exact structure of the initial hydrophilic pre-pore whose radius is defined as 0 ( $r = 0$ ), which may depend on lipid compositions. Figure 4(aI) and Fig. 4(bI) are the illustration of the two structures of the initial pre-pore among many possible structures. Figure 4(aI) is similar to the structure of the initial pre-pore obtained by the MD simulations,<sup>31</sup> where the lipid packing in the rim is high and the structure of lipid is a little distorted. By contrast, Fig. 4(bI) shows a more relaxed structure of the rim, where the lipid packing in the rim is lower than that of Fig. 4(aI), which is similar to the structure of the final pre-pore [Figs. 4(aII) and 4(bII)]. The definition of the radius of the hydrophilic pre-pore has some arbitrariness owing to the thickness ( $R_0$  in Fig. 4) of the rim of the pre-pore (i.e., the rim is not a line, although in the following theory we approximate the rim as a line), which depends on the researchers.<sup>7–12,29–31</sup> When we define the radius of the pre-pore,  $r$ , using the innermost rim for simplification, the  $r$  is equal to the separation between the rightmost edge line defined in the initial pre-pore [line A in Figs. 4(aI) and 4(bI)] and the central line of the pre-pore [line O in Figs. 4(aII) and 4(bII)]. The radius of the water channel greatly depends on the initial structure of pre-pores. Here we adopted the structure shown in Fig. 4(aI) as the initial pre-pore. As the radius of the pre-pore increases, the lipid packing

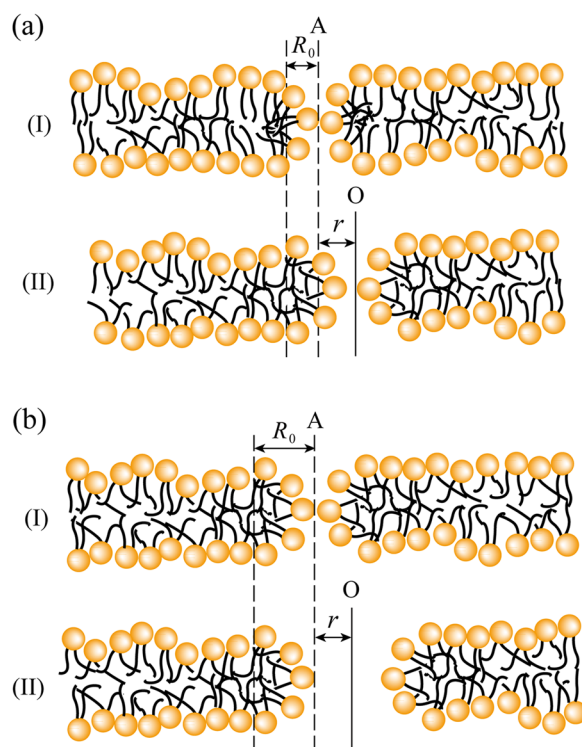


FIG. 4. Illustration of two structures of hydrophilic pre-pores. Here, we defined the radius of the pre-pore,  $r$ , using the innermost rim for simplification, and thus, the  $r$  is equal to the separation between the rightmost edge line defined in the initial pre-pore (line A) and the central line of the pre-pore (line O). (a) (I) A structure of the initial pre-pore ( $r = 0$ ), where the lipid packing in the rim is high and the structure of lipid is a little distorted. (II) The structure of the pre-pore with radius of  $r$ . The lipid packing in the rim becomes lower than that of the initial structure shown in (I) and the structure of the rim becomes relaxed, and hence the thickness of the rim increases. As a result, the radius of the water channel at the center of the pre-pore becomes much smaller than that of the pre-pore. (b) (I) A structure of the initial pre-pore ( $r = 0$ ) with a more relaxed structure of the rim, where the lipid packing in the rim is lower. (II) The structure of the pre-pore with radius of  $r$ . The structure and the thickness of the rim are the same as those of the initial structure. As a result, the radius of the pre-pore is equal to that of the water channel.

in the rim becomes lower and the structure of the rim becomes relaxed, which increases the thickness of the rim [Fig. 4(aII)]. Therefore, the radius of the water channel at the center of the pre-pore becomes much smaller than that of the pre-pore. This structural change of the rim of the pre-pore is supported by the results of the MD simulations.<sup>31</sup> However, if we use the structure shown in Fig. 4(bI) for the initial pre-pore, the radius of the pre-pore is always equal to that of the water channel.

According to the theory of tension-induced pore formation in lipid bilayers,<sup>9–12</sup> production of a pre-pore with radius  $r$  in the charged bilayer would change the total free energy of the system by the free energy of a pre-pore,  $U(r)$ , which consists of three factors. The first term ( $2\pi r\Gamma$ ) is the line free energy at the rim of a pre-pore due to the line tension,  $\Gamma$ , of the pre-pore edge (i.e., the line free energy per unit length of a pre-pore in a lipid membrane), which favors decrease in the size of the pre-pore. The second term ( $-\pi\sigma r^2$ ) is associated with tension,  $\sigma$ , due to the decrease in elastic energy of the bilayer. The third term ( $-\pi B r^2$ ) is due to the electrostatic interactions (the second and the third terms favor an increase in the size of pre-pore).

Hence, the  $U(r)$  can be described as

$$U(r) = 2\pi\Gamma r - \pi(\sigma + B)r^2 + U_0, \quad (3)$$

where  $U_0$  is the nucleation free energy required to form a hydrophilic pre-pore<sup>9,32</sup> and  $B$  is a term reflecting electrostatic interactions arising from surface charges.  $B$  can be written as<sup>33</sup>

$$B = \left\{ 4\Omega \left[ \frac{1-q}{p} + \ln(p+q) \right] \frac{kT}{e} - \frac{\Omega^2}{\varepsilon_w \varepsilon_0} a^2 \frac{h}{2} \right\}, \quad (4)$$

where  $\Omega$  is the surface charge density of the membrane,  $\varepsilon_w$  is the relative dielectric constant of water,  $\varepsilon_0$  is the permittivity of free space,  $h$  is the bilayer thickness,  $k$  is the Boltzmann constant,  $T$  is the temperature, and  $p$  and  $q$  are defined by the formulae  $p = 2\pi\lambda_B X / \kappa A_0$  and  $q = \sqrt{1+p^2}$  (where  $X$  is the molar fraction of negatively charged PG in the lipid bilayer,  $\lambda_B$  is the Bjerrum length in water,  $\lambda_B = e^2 / 4\pi\kappa T \varepsilon_0 \varepsilon_w$ ,  $e$  is the elementary charge,  $A_0$  is the cross-sectional area per lipid molecule in the bilayer under no tension, and  $1/\kappa$  is the Debye length).  $U(r)$  has a maximum, i.e., the activation energy of pore formation,  $U_a$ , at the critical radius,  $r_c = \Gamma / (\sigma + B)$ , as follows:<sup>9</sup>

$$U_a = U_0 + \pi\Gamma^2 / (\sigma + B). \quad (5)$$

The values of the parameters were determined by the best fit to the data of the dependence of experimentally determined  $U_a$  on tension  $\sigma$  obtained previously;<sup>9</sup>  $B = 1.8$  mN/m,  $U_0 = 9.0$  pN-nm ( $= 2.2 kT$ ), and  $\Gamma = 12.4$  pN. We can obtain the equation of the rate constant of tension-induced pore formation,  $k_p$ , using the standard Arrhenius equation with the activation energy expressed by Eq. (5) with the values of the parameters above, which has been well fit to the other independent experimental data (i.e., the tension dependence of  $k_p$ ) using only one parameter (the frequency factor,  $A_F$ ).<sup>9</sup> This result supported the validity of the theory and Eq. (5). Figure 5 shows the free energy landscape,  $U(r)$ , for various tensions. Notably, the radius of the pre-pore,  $r$ , varies rapidly with time due to thermal fluctuation. When  $r$  is less than  $r_c$ , the pre-pore closes quickly (i.e., no pore formation), but when  $r$  is above  $r_c$ , pore formation occurs. Equation (5) and Fig. 5 indicate that  $U_a$  decreases with tension. The initial slope of  $U(r)$  decreases

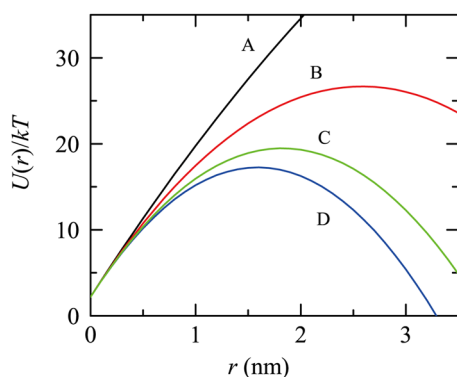


FIG. 5. Free energy profile of a hydrophilic pre-pore with radius  $r$ ,  $U(r)$ , for various tensions. Curve A:  $\sigma = 0$ , B: 3.0, C: 5.0, and D: 6.0 mN/m.  $U(r)$  was determined based on Eq. (3) using  $B = 1.8$  mN/m,  $U_0 = 2.2 kT$ , and  $\Gamma = 12.4$  pN. Here we assumed that the radius of initial hydrophilic pre-pore is zero.

with a decrease in  $U_{\max}$ , and hence the rate of hydrophilic pre-pore formation increases with increasing  $\sigma$ . We can reasonably infer that lipid molecules can diffuse laterally through the wall of the pre-pore, which may explain the experimental observation that the  $k_{FF}$  of the lipids increased with tension.

Figure 5 indicates that the critical radius  $r_c$  of the pre-pore at 5–6 mN/m is  $\sim 1.5$  nm. The corresponding diameter is larger than the size of AF647 [its Stokes-Einstein radius is  $\sim 0.9$  nm based on the size (0.88 nm) of the similar compound, AF647 succinimidyl ester<sup>34</sup>], and hence one may consider that AF647 can permeate through the pre-pores. However, our experimental results indicated that the leakage of AF647 was not observed at  $\sigma = 5$ –6 mN/m. This apparent discrepancy can be explained as follows. Here we consider the structures shown in Fig. 4(a) as the pre-pore, where the radius of the water channel is much smaller than the radius of the prepore. Hence, even at the critical radius  $r_c$  of  $\sim 1.5$  nm, the radius of the water channel is smaller than the size of AF647. Even if we consider the structure shown in Fig. 4(b) as the pre-pore, we can explain this apparent discrepancy as follows. As we described above, the fluctuation of the radius of the pre-pore is induced by thermal energy, and hence its radius rapidly fluctuated. Moreover, the free energy of the pre-pore  $U(r)$  is large at around the critical radius. Therefore, we can reasonably infer that the probability of the appearance of a pre-pore with large radius near  $r_c$  is very low and the dwell time of a pre-pore at the large radius is very short, i.e., such a pre-pore forms very transiently. Moreover, the distance between the hydrophilic molecule, AF647, and the surface of the lipid bilayer is large owing to the repulsive interactions between hydrophilic surfaces.<sup>35</sup> Especially, the PG/PC bilayer, which was used as the lipid bilayer in the present work, has a highly negatively charged surface and AF647 has four negative charges and, thus, a large electrostatic repulsion between AF647 and the PG/PC membrane surface. Hence, the concentration of AF647 near the membrane surface greatly decreases because the distribution of AF647 in aqueous solution near the membrane follows the Boltzmann law.<sup>35</sup> Under this circumstance, if a pre-pore with a size larger than AF647 forms transiently, it is difficult for AF647 to permeate through the pre-pore. By contrast, peptides bound to lipid bilayers such as cell-penetrating peptides have an advantage to permeate through a transient pre-pore because these peptides do not have to spend time to reach the membrane surface.<sup>36</sup> Similarly, lipids located in the bilayer can permeate through a transient pre-pore.

The values of  $k_{FF}$  of NBD-LPE were smaller than those of NBD-PG. This distinction may reflect the location of the NBD group. The headgroup of NBD-LPE is larger than that of NBD-PG because the bulky NBD group is attached to the headgroup of NBD-LPE and to the hydrocarbon chain of NBD-PG. Therefore, a larger pre-pore size is required for the lateral diffusion of NBD-LPE (compared to that of NBD-PG) through the wall of the pre-pores.

Studies of the tension-induced pore formation in lipid bilayers using MD simulation have recently increased.<sup>30,31,37,38</sup> At the present stage of all-atom MD simulation, the time and the area of membrane that can be simulated are very limited,<sup>39</sup> and thus the fluctuation of the radius of a pre-pore has

not yet been modeled in MD simulations of lipid bilayers. Progress in MD simulation in the near future could provide new information on the formation of pre-pores in stretched bilayers and the transbilayer movement of lipids through the pre-pores.

## V. CONCLUSION

In this report, we found that the rate constant of the transbilayer movement of lipids increased with membrane tension without pore formation. We discussed the plausible mechanisms for this new phenomenon. As one of them, we hypothesized that the transbilayer movement of lipids occurs through hydrophilic pre-pores.

## ACKNOWLEDGMENTS

This work was supported in part by a Grant-in-Aid for Scientific Research (B) (Grant No. 15H04361) from the Japan Society for the Promotion of Science (JSPS) to M.Y.

- <sup>1</sup>O. Sandre, L. Moreaux, and F. Brochard-Wyart, *Proc. Natl. Acad. Sci. U. S. A.* **96**, 10591 (1999).
- <sup>2</sup>E. Evans, V. Heinrich, F. Ludwig, and W. Rawicz, *Biophys. J.* **85**, 2342 (2003).
- <sup>3</sup>T. Portet and R. Dimova, *Biophys. J.* **99**, 3264 (2010).
- <sup>4</sup>S. U. A. Shibly, C. Ghatak, M. A. S. Karal, M. Moniruzzaman, and M. Yamazaki, *Biophys. J.* **111**, 2190 (2016).
- <sup>5</sup>F. Sachs, *Physiology* **25**, 50 (2010).
- <sup>6</sup>E. Karatekin, O. Sandre, H. Guitouni, N. Borghi, P.-H. Puech, and F. Brochard-Wyart, *Biophys. J.* **84**, 1734 (2003).
- <sup>7</sup>E. Evans and B. A. Smith, *New J. Phys.* **13**, 095010 (2011).
- <sup>8</sup>V. Levadny, T. Tsuboi, M. Belaya, and M. Yamazaki, *Langmuir* **29**, 3848 (2013).
- <sup>9</sup>M. A. S. Karal, V. Levadny, and M. Yamazaki, *Phys. Chem. Chem. Phys.* **18**, 13487 (2016).
- <sup>10</sup>J. D. Litster, *Phys. Lett. A* **53**, 193 (1975).
- <sup>11</sup>R. W. Glaser, S. L. Leikin, L. V. Chernomordik, V. F. Pastushenko, and A. I. Sokirko, *Biochim. Biophys. Acta* **940**, 275 (1988).
- <sup>12</sup>G. Fuertes, D. Giménez, S. Esteban-Martín, O. L. Sánchez-Muñoz, and J. A. Salgado, *Eur. Biophys. J.* **40**, 399 (2011).
- <sup>13</sup>K. C. Melikov, V. A. Frolov, A. Shcherbakov, A. V. Samsonov, Y. A. Chizmadzhev, and L. V. Chernomordik, *Biophys. J.* **80**, 1829 (2001).
- <sup>14</sup>H. M. McConnell and R. D. Kornberg, *Biochemistry* **10**, 1111 (1971).
- <sup>15</sup>R. Homan and H. J. Pownall, *Biochim. Biophys. Acta, Biomembr.* **938**, 155 (1988).
- <sup>16</sup>W. C. Wimley and T. E. Thompson, *Biochemistry* **29**, 1296 (1990).
- <sup>17</sup>J. Bai and R. E. Pagano, *Biochemistry* **36**, 8840 (1997).
- <sup>18</sup>M. J. Moreno, L. M. B. B. Estronca, and W. L. C. Vaz, *Biophys. J.* **91**, 873 (2006).
- <sup>19</sup>M. Hasan, M. A. S. Karal, V. Levadny, and M. Yamazaki, *Langmuir* **34**, 3349 (2018).
- <sup>20</sup>Y. Tamba, H. Terashima, and M. Yamazaki, *Chem. Phys. Lipids* **164**, 351 (2011).
- <sup>21</sup>W. Rawicz, K. C. Olbrich, T. J. McIntosh, D. Needham, and E. Evans, *Biophys. J.* **79**, 328 (2000).
- <sup>22</sup>E. I. Kitsioulis, G. Nakos, and M. E. Lekka, *J. Lipid Res.* **40**, 2346 (1999).
- <sup>23</sup>M. A. S. Karal, J. M. Alam, T. Takahashi, V. Levadny, and M. Yamazaki, *Langmuir* **31**, 3391 (2015).
- <sup>24</sup>M. S. C. Abreu, M. J. Moreno, and W. L. C. Vaz, *Biophys. J.* **87**, 353 (2004).
- <sup>25</sup>J. L. MacCallum, W. F. D. Bennett, and D. P. Tielman, *Biophys. J.* **101**, 110 (2011).
- <sup>26</sup>H. S. Muddana, R. R. Gullapalli, E. Manias, and P. J. Butler, *Phys. Chem. Chem. Phys.* **13**, 1368 (2011).
- <sup>27</sup>A. S. Reddy, D. T. Warshaviak, and M. Chachisvillias, *Biochim. Biophys. Acta* **1818**, 2271 (2012).
- <sup>28</sup>P. J. Butler, G. Norwich, S. Weinbaum, and S. Chien, *Am. J. Physiol.: Cell. Physiol.* **280**, C962 (2001).
- <sup>29</sup>S. A. Akimov, P. E. Volynsky, T. R. Galimzyanov, P. I. Kuzmin, K. V. Pavlov, and O. V. Batishchev, *Sci. Rep.* **7**, 12152 (2017).
- <sup>30</sup>T. V. Tolpekina, W. K. den Otter, and W. J. Briels, *J. Chem. Phys.* **121**, 12060 (2004).
- <sup>31</sup>J. Wohlert, W. K. den Otter, O. Edholm, and W. J. Briels, *J. Chem. Phys.* **124**, 154905 (2006).
- <sup>32</sup>M. A. S. Karal and M. Yamazaki, *J. Chem. Phys.* **143**, 081103 (2015).
- <sup>33</sup>M. A. S. Karal, V. Levadny, T. Tsuboi, M. Belaya, and M. Yamazaki, *Phys. Rev. E* **92**, 012708 (2015).
- <sup>34</sup>C. Jung, J. Lee, M. Kang, and S. W. Kim, *J. Korean Phys. Soc.* **65**, 1083 (2014).
- <sup>35</sup>J. N. Israelachvili, *Intermolecular and Surface Forces*, 2nd ed. (Academic Press, New York, 1992).
- <sup>36</sup>M. Z. Islam, S. Sharmin, M. Moniruzzaman, and M. Yamazaki, *Appl. Microbiol. Biotechnol.* **102**, 3879 (2018).
- <sup>37</sup>D. P. Tieleman, H. Leontiaudou, A. E. Mark, and S.-J. Marrink, *J. Am. Chem. Soc.* **125**, 6382 (2003).
- <sup>38</sup>T. Shigematsu, K. Koshiyama, and S. Wada, *Sci. Rep.* **5**, 15369 (2015).
- <sup>39</sup>I. Buch, M. J. Harvey, T. Giorgino, D. P. Anderson, and G. D. Fabritiis, *J. Chem. Inf. Model.* **50**, 397 (2010).